

Distance-based Local Geocasting in Multi-hop Wireless Networks

Quan Jun Chen, Salil S. Kanhere, Mahbub Hassan, Yuvraj Krishna Rana
School of Computer Science and Engineering,
The University of New South Wales, Sydney, Australia,
Email: {quanc, salilk, mahbub, yran496}@cse.unsw.edu.au

Abstract—Geocasting uses location information to disseminate messages within a specified geographic area. However, in some applications, it is not feasible for the nodes to be able to determine their location coordinates. In this paper, we propose a novel *distanced-based* approach for *local geocasting* to address this problem. In local geocasting, source node is interested in spread messages within a local area around itself. We exploit the relationship between radius of local area and the expected hop count in a multi-hop wireless network with uniformly distributed nodes. We estimate the minimum number of hops required to cover all of the nodes within the given local geocasting area. The hop count is then used as hop limit to restrict flooding. We theoretically analyze the average number of rebroadcast messages in the proposed approach and the analytical model is validated by the statistic results. We further conduct a simulation-based comparison between distance-based local geocasting and traditional local geocasting. The results show that our approach can achieve a similar performance as that of traditional local geocasting.

I. INTRODUCTION

Flooding is one of the simplest strategy for disseminating messages globally in a wireless multi-hop network. In flooding, the source node broadcasts the message to all of its neighbouring nodes. These neighbours in turn relay the message to their respective neighbours and so on until the message has been propagated to the entire network (This is commonly known as *blind flooding*). Due to its simplicity, flooding has been widely used in many applications and network protocols. For example, several reactive routing protocols such as AODV [1], DSR [2] and ZRP [3] utilize flooding for route discovery. Service discovery protocols [4] also flood service requests within the network to locate nodes that offer the requested services. Although straightforward, flooding is far from optimal and generates a high number of redundant messages and consumes valuable resources such as bandwidth and battery power. In addition, if the flooded messages are control packets (as is the case with routing protocols), they may collide with data packets consequently affecting the packet delivery and delay. In recent years, several schemes [5], [6], [7], [8] have been proposed to optimise flooding and reduce the number of redundant messages. The approaches vary from using probabilistic flooding wherein each nodes broadcasts a message with a certain probability [6] to using local topology knowledge before making a broadcasting decision [8].

Geocasting [9] is a special case of flooding wherein the scope of the flooded message is bounded to a specific ge-

ographic area. In other words, the message only has to be delivered to all nodes that are within the specified geographical region. Network-wide blind flooding is obviously not attractive for this purpose. In naive geocasting [9], a *forwarding region* is formed which encompasses the source node and the target area and blind flooding is employed therein. Though this achieves the desired objective, it leads to excessive broadcasts in the surrounding areas of the target. Several schemes have been proposed [10], [11], which limit the size of the forwarding region and consequently reduce the redundant geocast messages. However, all these geocasting protocols require that each node in the network is aware of its precise location coordinates. The location information is necessary for a node to decide if it should continue to broadcast a received message.

In this paper, we focus on local geocasting, wherein a node is interested in disseminating messages to all nodes located within a certain distance D from it. In other words, the geocast region is a circle of radius D centered at the message source. There are several applications, where this communication primitive of localized geocasting is desirable. Since energy is a critical resource in sensor nodes, most large-scale sensor network deployments dynamically active and deactivate sensor nodes. If an active sensor node detects a high priority event (e.g: fire outbreak), it is required to wake up other nodes within its vicinity to confirm this occurrence and also to relay the information to the base station. Disaster recovery workers will often require broadcasting of warning or help messages to other crew within the immediate vicinity. Further, future Intelligent Transportation System (ITS) [12] road safety applications require vehicles to broadcast warning messages to other vehicles within a certain neighborhood to prevent accidents or to warn of traffic conditions.

Note that any variant of geocasting (similar to those described earlier) could be used for this purpose. However, all of these protocols require that each node is aware of its position coordinates. Equipping each node with a GPS device may not be always feasible especially in low-cost devices such as sensor. Further, GPS is not effective in indoor environments. GPS-less localization schemes [13] can be used to enable nodes to determine their physical locations. However, these schemes are prone to introducing reasonably large errors in the position estimates, which can adversely effect message delivery in geocasting. A local geocasting scheme, which does not require any location information is thus desirable.

In this paper, we propose a novel distance-based local geocasting scheme for a multi-hop wireless network, which does not require that the nodes know their geographic location information. Our scheme is based on our earlier analysis [14], wherein we have identified a relationship between the physical distance separating two communicating nodes in a multi-hop network and the corresponding hop count (i.e. the number of hops). Since the local geocast radius d is known a priori, our proposed scheme uses the aforementioned relationship to determine the corresponding *hop count radius* \hat{h} , which is then used as the TTL (Time to Live) to restrict the flooding of the message to within the desired geocasting area. \hat{h} should satisfy the following two constraints: (i) It should ensure that the message can reach all nodes within distance d from the source with a high probability and (ii) It should be the minimum number of hops that can achieve the first goal, so as to minimize the propagation of the message to beyond the target region. Note that we resort to blind flooding within the target geocasting region. More elaborate schemes such as those in (described earlier) can be used to further reduce the broadcast messages.

We theoretically analyze the performance of our approach and prove that in a network consisting of N nodes the proposed scheme requires only $0.42N$ number of broadcast messages on average. We validate our analytical model using statistic results from randomly generated networks. We also conduct a simulation-based performance evaluation of our scheme and compare the results to network-wide flooding and geocasting. The results show that the proposed local geocasting scheme can reduce the redundant broadcasts by up to 40% in comparison with network-wide flooding. A similar reduction in MAC-layer collisions is also observed. Moreover, the results reveal that the performance of our proposed scheme is similar to that of traditional geocasting. Thus without imposing the requirement that each node knows its physical location, our scheme demonstrates similar performance.

The rest of the paper is organized as follows. In Section II, we elaborate on the estimation of the hop count radius given the required geocasting radius. Then we theoretically evaluate the performance of our approach in Section III. In Section IV, we discuss the simulation-based comparisons. Finally, we conclude the paper in Section V.

II. ESTIMATION OF THE HOP COUNT RADIUS

In our earlier work [14], we have proposed a markov chain based mathematical model to compute the hop count along the shortest hop path given the source-to-destination distance for a multi-hop network with uniformly distributed nodes. The model also enables us to calculate the probability mass function (*pmf*) for the hop count. In this section we only provide the pertinent formulas, interested readers are referred to [14] for further details.

Let D represent the distance between the source and destination. Note that, for the case of local geocasting, D denotes the geocasting distance. Let H denote the corresponding hop count and R represent the radio range. According to Theorem

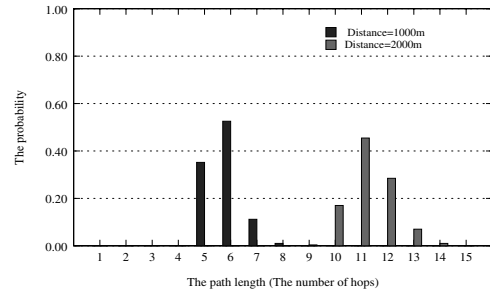


Fig. 1. Probability mass function of the hop count

5 defined in [14], the probability distribution of hop count is given by the following,

$$P(H = h|D = i) = \begin{cases} 1 & \text{if } 0 < i \leq R \text{ and } h = 1, \\ 0 & \text{if } 0 < i \leq R \text{ and } h > 1, \\ 0 & \text{if } i > R \text{ and } h < \lceil \frac{i}{R} \rceil, \\ \frac{\sum_{j=i-R|\varepsilon}^{i-\varepsilon} P(H=h-1|D=j)P_{i,j}}{1-P_{i,i}} + \frac{\sum_{j=i+\varepsilon|e}^{i+R} P(H=h-1|D=j)P_{i,j}}{1-P_{i,i}} & \text{otherwise,} \end{cases} \quad (1)$$

where $P_{i,j}$ is the transition probability from state i to j and ε is the state interval (i.e. the quantization interval). Note that, in our model the state is defined as the euclidean distance between the current forwarding node to the destination. $P_{i,j}$ is given by Theorem 2 in [14], as below.

$$P_{i,j} = \begin{cases} 1 & \text{if } i \leq R \text{ and } j = 0, \\ 0 & \text{if } i \leq R \text{ and } j > 0, \\ \sum_{k=1}^{\bar{m}} \binom{\bar{m}}{k} \left(\frac{A_{i,j+\varepsilon} - A_{i,j}}{\pi R^2} \right)^k \left(1 - \frac{A_{i,j+\varepsilon}}{\pi R^2} \right)^{\bar{m}-k} & \text{if } i > R \text{ and } i - R \leq j < i, \\ \sum_{k=1}^{\bar{m}} \binom{\bar{m}}{k} \left(\frac{A_{i,j} - A_{i,j-\varepsilon}}{\pi R^2} \right)^k \left(1 - \frac{A_{i,j}}{\pi R^2} \right)^{\bar{m}-k} & \text{if } i > R \text{ and } i < j \leq i + R, \\ 0 & \text{if } i > R \text{ and } (i = j \text{ or } j < i - R \text{ or } j > i + R), \end{cases} \quad (2)$$

where \bar{m} is the average number of neighbors. If N denotes the total number of nodes in the network and A represents the area of network then,

$$\bar{m} = (N - 1) \frac{\pi R^2}{A} \quad (3)$$

Further, $A_{i,j}$ is defined as:

$$A_{i,j} = R^2 \arccos \frac{i^2 + R^2 - j^2}{2iR} + j^2 \arccos \frac{i^2 + j^2 - R^2}{2ij} - \frac{\sqrt{(R+i+j)(R+i-j)(R-i+j)(i+j-R)}}{2} \quad (4)$$

By recursively calculating the above equations, we can compute the probability mass function of the hop count given a distance. For example, if $N = 115$, $A = 1500 * 1500m^2$, $R = 250$, $\varepsilon = 5$, Fig. 1 plots the *pmf* of the hop count for two values of D : 1000m and 2000m, respectively.

Recall that we want to ensure that messages can reach all nodes inside the target geocast area, which is a circle of distance d centered at the message source, with a certain

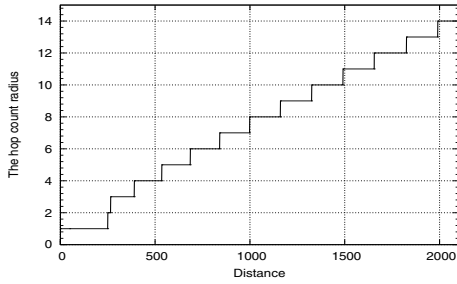


Fig. 2. The hop count radius $\hat{h}(d)$

probability α . α is a system design parameter and for most applications is expected to be close to 1. Let $\hat{h}(d)$ denote the hop count radius corresponding to the distance d . We have,

$$\hat{h}(d) = \underset{\hat{h}}{\operatorname{argmin}} \{P(H \leq \hat{h} | D = d) \geq \alpha\} \quad (5)$$

For instance, in the example of Fig. 1, if $\alpha = 0.99$, then $\hat{h}(1000) = 8$ and $\hat{h}(2000) = 14$. Fig. 2 illustrates $\hat{h}(d)$ as a function of d for the same network parameters as those used in Fig. 1. $\hat{h}(d)$ is then used as the TTL (Time to Live) in the geocast message. Each node decrements the TTL by one. If the TTL equals zero, the node drops the packet. Otherwise the node broadcasts the packet to its neighbours. Thus, this ensures that the message is distributed only to those nodes that are within the desired geocasting area.

To evaluate the effectiveness of our scheme it is important to know the actual distance within which nodes rebroadcast the message if a TTL of $\hat{h}(d)$ is used. As such, we define the *actual flooding distance* as the radius of area within which nodes will rebroadcast messages. Note that the recipient of last hop does not rebroadcast messages. Only nodes within hop count $\hat{h}(d) - 1$ from source are involved in rebroadcasting. We also introduce a new parameter called the average progress per hop, which measures the distance covered by each hop. In [14], average progress per hop has been formulated as λR , where λ is given by,

$$\lambda = 1 - \int_{-1}^1 \left(1 - \frac{\arccos(t) - t\sqrt{1-t^2}}{\pi}\right)^m dt \quad (6)$$

Obviously with the hop count radius of $\hat{h}(d)$, the actual flooding distance for the geocast message is, $\hat{d} = \lambda R(\hat{h}(d) - 1)$. Since $\hat{h}(d)$ is an integer, \hat{d} is also an integral multiple of λR .

III. PERFORMANCE ANALYSIS

In this section, we theoretically analyze the performance of the proposed local geocasting scheme. We evaluate the average number of broadcast messages generated by our strategy denoted by \hat{N} for a hop count radius of \hat{h} .

We have made the following assumptions in our analysis: 1) Nodes are uniformly distributed in a square network of dimension $l * l$. 2) The source of the geocast messages are randomly selected from all nodes, which also implies that that sources are uniformly located in the network. 3) The

probability distribution of flooding distance d satisfies the assumption that \hat{h} is uniformly distributed from 1 to $\lfloor \frac{l}{\lambda R} \rfloor + 1$. 4) We use blind flooding within the geocast region. 5) We assume an ideal MAC and PHY layer and that no packets are lost.

Note that, we distinguish between flooding coverage and the effective flooding coverage. Flooding coverage is the circular region in which the center is the geocasting source and radius is the actual flooding distance, i.e. \hat{d} . In some cases when flooding source is located near network border, parts of flooding coverage may not cover any nodes, as illustrated in Fig. 3. Therefore we define "effective flooding coverage" as the intersection area between the square network and the flooding coverage. Intuitively, the number of broadcasting messages is equal to the number of nodes that reside in effective flooding coverage. Since nodes are uniformly distributed, the number of nodes within the effective flooding coverage is proportional to the area of this region, $\bar{\delta}$.

Let $\delta(\hat{h})$ be the effective flooding coverage given the hop count radius \hat{h} . We can calculate $\delta(\hat{h})$ by employing a geometric approach. Since \hat{h} is uniformly distributed from 1 to $\lfloor \frac{l}{\lambda R} \rfloor + 1$, by the law of total probability, we can calculate the average effective flooding coverage over all possible values of \hat{h} . We have,

Theorem 1: If \hat{h} is the hop count radius corresponding to a geocasting distance of d , and the probability distribution of d satisfies the assumption that \hat{h} is uniformly distributed within $[1, \lfloor \frac{l}{\lambda R} \rfloor + 1]$, where λ is defined in Equation (6), then the average number of broadcast messages, \hat{N} has an upper bound given by,

$$\hat{N} < \frac{N}{l^4} \frac{1}{\lfloor \frac{l}{\lambda R} \rfloor + 1} \left(\sum_{\hat{h}=2}^{\lfloor \frac{l}{2\lambda R} \rfloor + 1} \left(9\hat{d}^4 + 4(l - 2\hat{d})(\pi - 1 + \frac{1}{4\pi})\hat{d}^3 + \pi\hat{d}^2(l - 2\hat{d})^2 \right) + \sum_{\hat{h}=\lfloor \frac{l}{2\lambda R} \rfloor + 2}^{\lfloor \frac{l}{\lambda R} \rfloor + 1} (2l - \hat{d})^2 \hat{d}^2 \right) \quad (7)$$

where $\hat{d} = \lambda R(\hat{h} - 1)$.

Proof: As discussed earlier, the average number of broadcast messages \hat{N} is proportional to the area of average effective flooding coverage $\bar{\delta}$. Hence, we have,

$$\hat{N} = \bar{\delta} \frac{N}{l^2}. \quad (8)$$

Recall that $\bar{\delta}$ is the average value over $\delta(\hat{h})$. Since \hat{h} is an integer and uniformly distributed from 1 to $\lfloor \frac{l}{\lambda R} \rfloor + 1$, we have,

$$\bar{\delta} = \frac{1}{\lfloor \frac{l}{\lambda R} \rfloor + 1} \left(\sum_{\hat{h}=1}^{\lfloor \frac{l}{\lambda R} \rfloor + 1} \delta(\hat{h}) \right) \quad (9)$$

To compute $\delta(\hat{h})$, we consider two ranges of \hat{h} due to the different geometric shape of $\delta(\hat{h})$: Case A) when $1 \leq \hat{h} \leq \lfloor \frac{l}{2\lambda R} \rfloor + 1$ and Case B) when $\lfloor \frac{l}{2\lambda R} \rfloor + 2 \leq \hat{h} \leq \lfloor \frac{l}{\lambda R} \rfloor + 1$.

We evaluate the two cases separately:

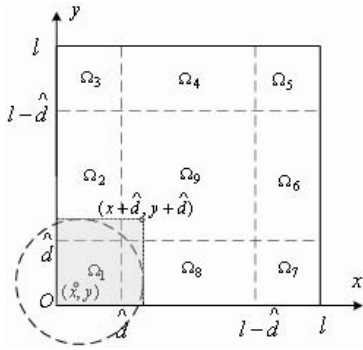


Fig. 3. The example of effective flooding coverage for case A

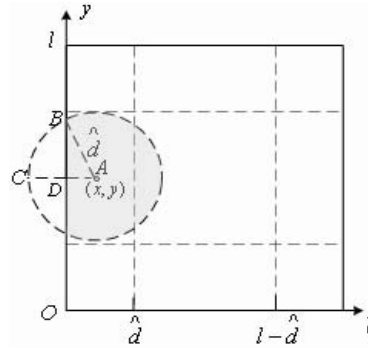


Fig. 4. The example of effective flooding coverage for case A

A. When $1 \leq \hat{h} \leq \lfloor \frac{l}{2\lambda R} \rfloor + 1$

As illustrated in Fig. 3 we put the square network in a two dimensional coordinate system, where the origin lies in the bottom left corner of the network(O). Note that the source is uniformly located in THE network area. The probability density function of the source location is given by,

$$f(x, y) = \frac{1}{l^2}, 0 \leq x \leq l, 0 \leq y \leq l, \quad (10)$$

Let $\delta_{(x,y)}(\hat{d})$ be the area of effective flooding coverage given that the flooding source is located at (x, y) and the actual flooding distance is \hat{d} . According to the different shape of $\delta_{(x,y)}(\hat{d})$, we split (x, y) into nine subcases, as marked from Ω_1 to Ω_9 in Fig. 3. Note that in the square network, areas $\Omega_1, \Omega_3, \Omega_5$ and Ω_7 are symmetric. In addition, the areas $\Omega_2, \Omega_4, \Omega_6$ and Ω_8 are also symmetric. Thus we only need discuss the following three sub-cases: 1) source is located in the square area Ω_1 ; 2) source is located the rectangular area Ω_2 , 3) source is located in the square area Ω_9 . Thus the average effective flooding coverage $\delta(\hat{h})$ over all possible (x, y) is ,

$$\begin{aligned} \delta(\hat{h}) &\stackrel{\hat{d}=\lambda R(\hat{h}-1)}{\implies} \int_0^l \int_0^l \delta_{(x,y)}(\hat{d}) f(x, y) dx dy \\ &= \frac{1}{l^2} \left(4 \oint \oint_{\Omega_1} \delta_{(x,y)}(\hat{d}) dx dy + 4 \oint \oint_{\Omega_2} \delta_{(x,y)}(\hat{d}) dx dy \right. \\ &\quad \left. + \oint \oint_{\Omega_9} \delta_{(x,y)}(\hat{d}) dx dy \right) \end{aligned} \quad (11)$$

For subcase 1), where the source is located in the area of $\Omega_1: x \in [0, \hat{d}]$ and $y \in [0, \hat{d}]$, we use the shadow rectangular area as illustrated in Fig. 3 to approximate $\delta_{(x,y)}(\hat{d})$. Obviously, the shadow rectangular area is slightly bigger than $\delta_{(x,y)}(\hat{d})$. We have,

$$\begin{aligned} &\oint \oint_{\Omega_1} \delta_{(x,y)}(\hat{d}) dx dy \\ &< \int_0^{\hat{d}} \int_0^{\hat{d}} (x + \hat{d})(y + \hat{d}) dx dy = \frac{9\hat{d}^4}{4} \end{aligned} \quad (12)$$

For sub-case 2), where the source is within the area of $\Omega_2: x \in [0, \hat{d}]$ and $y \in [\hat{d}, l - \hat{d}]$, $\delta_{(x,y)}(\hat{d})$ is the shadow area illustrated in the circle of Fig. 4. Let $\delta_{\widehat{BAC}}$ be the area of sector \widehat{BAC} , and δ_{BAD} denote the area of triangle BAD . We

have,

$$\begin{aligned} \delta_{(x,y)}(\hat{d}) &= \pi \hat{d}^2 - 2(\delta_{\widehat{BAC}} - \delta_{BAD}) \\ &= \pi \hat{d}^2 - \left(\hat{d}^2 \arccos \frac{x}{\hat{d}} - x \sqrt{\hat{d}^2 - x^2} \right) \end{aligned} \quad (13)$$

Thus the integral over all possible (x, y) is given by,

$$\begin{aligned} \oint \oint_{\Omega_2} \delta_{(x,y)}(\hat{d}) dx dy &= \int_{\hat{d}}^{l-\hat{d}} \int_0^{\hat{d}} \delta_{(x,y)}(\hat{d}) dx dy \\ &= (l - 2\hat{d}) \int_0^{\hat{d}} \left(\pi \hat{d}^2 - \left(\hat{d}^2 \arccos \frac{x}{\hat{d}} - x \sqrt{\hat{d}^2 - x^2} \right) \right) dx \\ &\stackrel{x=\hat{d}t}{\implies} (l - 2\hat{d}) \left(\pi \hat{d}^3 - \hat{d}^3 \int_0^1 (\arccos(t) - \sqrt{1-t^2}) dt \right) \\ &= (\pi - 1 + \frac{1}{4\pi})(l - 2\hat{d})\hat{d}^3 \end{aligned} \quad (14)$$

For sub-case 3), where the source is within $\Omega_9: x \in [\hat{d}, l - \hat{d}], y \in [\hat{d}, l - \hat{d}]$, Obviously the effective flooding coverage equals to flooding coverage. Thus

$$\begin{aligned} \oint \oint_{\Omega_9} \delta_{(x,y)}(\hat{d}) dx dy &= \int_{\hat{d}}^{l-\hat{d}} \int_{\hat{d}}^{l-\hat{d}} \pi \hat{d}^2 dx dy \\ &= \pi \hat{d}^2 (l - 2\hat{d})^2 \end{aligned} \quad (15)$$

Combining equations (11) (12) (14) and (15), the average effective flooding coverage $\delta(\hat{h})$ for the first case when $1 \leq \hat{h} \leq \lfloor \frac{l}{2\lambda R} \rfloor + 1$ is,

$$\delta(\hat{h}) < \frac{1}{l^2} \left(9\hat{d}^4 + 4(l - 2\hat{d}) \left(\pi - 1 + \frac{1}{4\pi} \right) \hat{d}^3 + \pi \hat{d}^2 (l - 2\hat{d})^2 \right) \quad (16)$$

where $\hat{d} = \lambda R(\hat{h} - 1)$.

Now we proceed to the second case.

B. when $\lfloor \frac{l}{2\lambda R} \rfloor + 2 \leq \hat{h} \leq \lfloor \frac{l}{\lambda R} \rfloor + 1$

Similar to Case A, we split the whole network area into nine sub-areas as depicted in Fig. 5 and we only discuss three sub-cases since the rest are similar: 1) Source is located in Ω_1 , where $x \in [0, l - \hat{d}]$ and $y \in [0, l - \hat{d}]$; 2) Source is located in Ω_2 , where $x \in [0, l - \hat{d}]$ and $y \in [l - \hat{d}, \hat{d}]$, 3) Source is located in Ω_9 , where $x \in [l - \hat{d}, \hat{d}], y \in [l - \hat{d}, \hat{d}]$.

For subcase 1), similar to Case A, we use a slightly bigger rectangular area to approximate $\delta_{(x,y)}(\hat{d})$. Thus,

$$\begin{aligned} \oint \oint_{\Omega_1} \delta_{(x,y)}(\hat{d}) dx dy \\ < \int_0^{l-\hat{d}} \int_0^{l-\hat{d}} (x + \hat{d})(y + \hat{d}) dx dy = \frac{(l^2 - \hat{d}^2)^2}{4} \end{aligned} \quad (17)$$

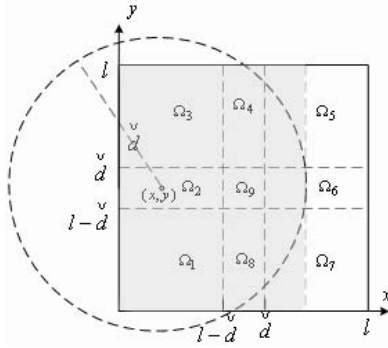


Fig. 5. The example of effective flooding coverage for case B

For subcase 2), we use the shadow area illustrated in Fig. 5 to approximate $\delta_{(x,y)}(\hat{d})$. Thus,

$$\oint \oint_{\Omega_2} \delta_{(x,y)}(\hat{d}) dx dy < \int_{l-\hat{d}}^{\hat{d}} \int_0^{l-\hat{d}} (x + \hat{d}) l dx dy = \frac{l^2 - \hat{d}^2}{2} (2\hat{d} - l) \quad (18)$$

Finally for subcase 3), the flooding coverage can almost cover whole network area. We use the whole network area to approximate $\delta_{(x,y)}(\hat{d})$. Thus,

$$\oint \oint_{\Omega_9} \delta_{(x,y)}(\hat{d}) dx dy < \int_{l-\hat{d}}^{\hat{d}} \int_{l-\hat{d}}^{\hat{d}} l^2 dx dy = (2\hat{d} - l)^2 l^2 \quad (19)$$

Combining the above three equations and equation (11), the average effective flooding coverage $\delta(\hat{d})$ for Case B, when $\lfloor \frac{l}{2\lambda R} \rfloor + 2 \leq \hat{h} \leq \lfloor \frac{l}{\lambda R} \rfloor + 1$ is,

$$\delta(\hat{h}) < \frac{1}{l^2} (2l - \hat{d})^2 \hat{d}^2 \quad (20)$$

Combining above two cases (A and B) and using equations (16), (20) and (9), we have,

$$\begin{aligned} \bar{\delta} &= \frac{1}{\lfloor \frac{l}{\lambda R} \rfloor + 1} \left(\sum_{\hat{h}=1}^{\lfloor \frac{l}{2\lambda R} \rfloor + 1} \delta(\hat{h}) + \sum_{\hat{h}=\lfloor \frac{l}{2\lambda R} \rfloor + 2}^{\lfloor \frac{l}{\lambda R} \rfloor + 1} \delta(\hat{h}) \right) \\ &< \frac{1}{(\lfloor \frac{l}{\lambda R} \rfloor + 1) l^2} \left(\sum_{\hat{h}=1}^{\lfloor \frac{l}{2\lambda R} \rfloor + 1} \left(9\hat{d}^4 + 4(l - 2\hat{d})(\pi - 1 + \frac{1}{4\pi})\hat{d}^3 + \pi\hat{d}^2(l - 2\hat{d})^2 \right) \right. \\ &\quad \left. + \sum_{\hat{h}=\lfloor \frac{l}{2\lambda R} \rfloor + 2}^{\lfloor \frac{l}{\lambda R} \rfloor + 1} (2l - \hat{d})^2 \hat{d}^2 \right) \end{aligned} \quad (21)$$

Finally, combining equations (8) and (21), the theorem is proved. ■

To understand the comparison of \hat{N} with N , we plot $\frac{\hat{N}}{N}$ in Fig. 6. The network size l varies from 4X to 12X of the radio range, R . The total number of nodes N is also correspondingly increased but the average number of neighbors has a constant value of 10. Fig. 6 shows that on average, no more than 50% of number of nodes are involved in rebroadcasting in our proposed local geocasting scheme.

In order to validate the analysis result illustrated in Fig. 6, we collect statistic results over randomly generated networks, where the parameters conform to the assumptions. For each network size, we randomly generate 10 networks and consider

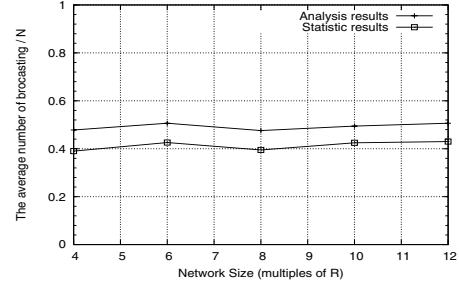


Fig. 6. The ratio of the average number of broadcast messages

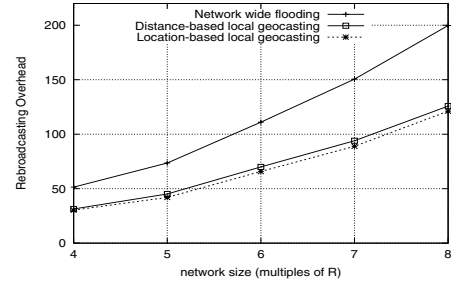


Fig. 7. Rebroadcasting overhead

all possible combinations of flooding sources and hop count radius ($\hat{h} \in [1, \lfloor \frac{l}{\lambda R} \rfloor + 1]$). For each combination of flooding source and \hat{h} , we count the number of nodes within hop count radius of $\hat{h} - 1$ from flooding source. The number of nodes represents the number of rebroadcast. Finally, we take the average value over the number of rebroadcasts. The simulation results are plotted in Fig. 6, which justify our analytical model.

IV. SIMULATION RESULTS

In this section, we present a simulation-based comparison among distance-based local geocasting, location-based local geocasting and network wide flooding. The simulations were conducted in NS-2 [15] with each experiment being run for 100 seconds. The results represented here are averaged over six runs, each using a different random seed. We vary network size from $1000m * 1000m$ to $2000m * 2000m$ and correspondingly, the total number of nodes is varied from 52 to 203. The nodes are uniformly distributed in the static networks. The radio range for each node was assumed to be 250 meters and thus the average number of neighbors is 10. We randomly select 10 sources from the network. Each source generates a flooding message with size of 64 bytes every second. The local geocasting radius (required flooding distance) is uniformly distributed from 0 to network size.

For our evaluations we use the following metrics: 1) Rebroadcasting overhead: This measures the ratio of total number of rebroadcasts to the number of flooding messages. 2) Reachability: This measures the percentage of nodes that reside in required geocasting area has received flooding messages. 3) MAC-layer collision: This measures the ratio of the total number of MAC-layer collisions to the number of flooding messages.

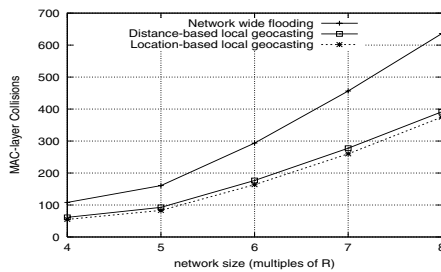


Fig. 8. MAC-layer collision

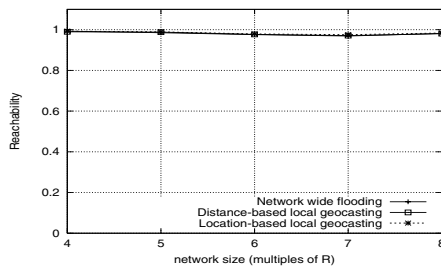


Fig. 9. Reachability

Fig. 7, 8 and 9 show that our proposed distance-based local geocasting can achieve very close performance as traditional location-based local geocasting. Compared to network wide flooding, local geocasting can reduce rebroadcasting overhead by 40% as illustrated in Fig. 7. Consequently, the MAC-layer collision is also decreased by 40%. Fig. 9 illustrates that all these schemes can cover near 99% of nodes within the required geocasting area, where the few uncovered nodes is mainly caused by packets lost due to the packets collision. We also conduct a set of simulations where the nodes move according to the random waypoint model [16] that has been widely used in the literature. Although random waypoint model does not result in a uniform distribution of the nodes [17], we found the simulations results are still similar to those presented here.

V. CONCLUSION

Local geocasting is an efficient mechanism to disseminate messages into a local area. However, the traditional location-based geocasting may not be applicable in some networks where the nodes are not affordable to equip with positioning devices. We propose an alternative approach that eliminates the requirement of location information. Based on the inherent relationship between distance and expected hop count, our approach estimates the hop count radius that can cover all of nodes in the required local geocasting area. We then use it as hop limit to restrict flooding. The rich set of simulations show that our distance-based local geocasting can achieve similar performance as that of location-based geocasting.

REFERENCES

- [1] C. E. Perkins and E. M. Royer. Ad-hoc on-demand distance vector routing (AODV). *WMCSA*, 00:90–100, 1999.
- [2] David B. Johnson, David A. Maltz, and Josh Broch. DSR: the dynamic source routing protocol for multihop wireless ad hoc networks. *Ad hoc networking*, pages 139–172, 2001.

- [3] Z. J. Haas and M. R. Pearlman. The zone routing protocol (ZRP) for ad hoc networks. draft-ietf-manet-zone-zrp-02.txt, 1999.
- [4] Z. Fan and E. G. Ho. Service discovery in mobile ad hoc networks. In *Proceedings of the 6th International Symposium on a World of Wireless Mobile and Multimedia Networks (WoWMoM2005)*, 2005.
- [5] S. Pleisch, M. Balakrishnan, K. Birman, and R. v. Renesse. MISTRAL: efficient flooding in mobile ad-hoc networks. In *MobiHoc '06: Proceedings of the seventh ACM international symposium on Mobile ad hoc networking and computing*, pages 1–12, 2006.
- [6] Q. Zhang and D. P. Agrawal. Dynamic probabilistic broadcasting in MANETs. *Journal of Parallel and Distributed Computing*, 65(2):220–233, February 2005.
- [7] R. Gandhi, S. Parthasarathy, and A. Mishra. Minimizing broadcast latency and redundancy in ad hoc networks. In *MobiHoc '03: Proceedings of the 4th ACM international symposium on Mobile ad hoc networking & computing*, pages 222–232. ACM Press, 2003.
- [8] B. Williams and T. Camp. Comparison of broadcasting techniques for mobile ad hoc networks. In *MobiHoc '02: Proceedings of the 3rd ACM international symposium on Mobile ad hoc networking & computing*, pages 194–205. ACM Press, 2002.
- [9] Y. Ko and N. H. Vaidya. Flooding-based geocasting protocols for mobile ad hoc networks. *Mobile Networks and Applications*, 7(6):471–480, December 2002.
- [10] Y. Ko and N. H. Vaidya. Geotora: A protocol for geocasting in mobile ad hoc networks. In *8th International Conference on Network Protocols (ICNP)*, November 2000.
- [11] L. Hughes and A. Maghsoudlou. An efficient coverage-based flooding scheme for geocasting in mobile ad hoc networks. In *Proceedings 20th International Conference on Advanced Information Networking and Applications (AINA2006)*, 2006.
- [12] Intelligent transportation system (ITS). <http://www.its.dot.gov/index.htm>.
- [13] N. Bulusu, J. Heidemann, and D. Estrin. Gps-less low cost outdoor localization for very small devices. *IEEE Personal Communications Magazine*, 7(5):28–34, October 2000.
- [14] Q. J. Chen, S. S. Kanhere, and M. Hassan. Modeling path length in wireless ad-hoc network. UNSW-CSE-TR-0617, <ftp://ftp.cse.unsw.edu.au/pub/doc/papers/UNSW/0617.pdf>, August 2006.
- [15] The vint project: Network simulator-ns 2. <http://www.isi.edu/nsnam/ns/>.
- [16] J. Broch, D. A. Maltz, D. B. Johnson, Y.-C. Hu, and J. Jetcheva. A performance comparison of multi-hop wireless ad hoc network routing protocols. In *MobiCom '98: Proceedings of the 4th annual ACM/IEEE international conference on Mobile computing and networking*, pages 85–97. ACM Press, 1998.
- [17] C. Bettstetter, H. Hartenstein, and X. Prez-Costa. Stochastic properties of the random waypoint mobility model. *Wireless Networks*, 10(5):555–567, September 2004.